

*Dedicated to the memory of  
Academician Bogdan C. Simionescu (1948–2024)*

## SUSTAINABLE PATHWAYS FOR POLY(ETHYLENE BRASSYLATE) SYNTHESIS

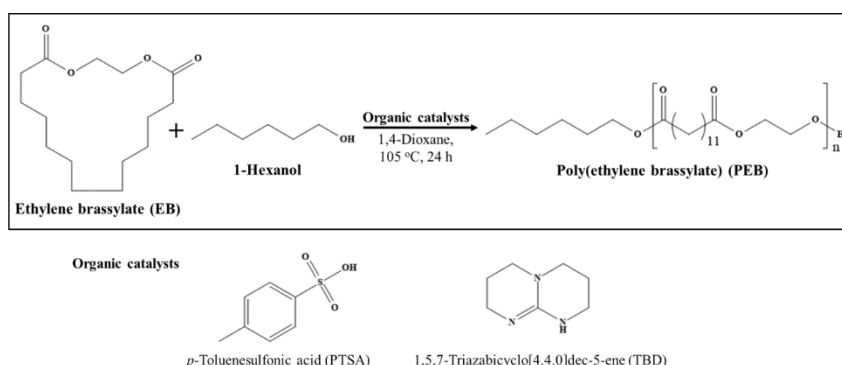
Bianca-Elena-Beatrice CRETU,<sup>a</sup> Alina Gabriela RUSU,<sup>a</sup> Daniel TIMPU<sup>b</sup> and Loredana E. NITA<sup>a,\*</sup>

<sup>a</sup> Department of Natural Polymers, Bioactive and Biocompatible Materials, Petru Poni Institute of Macromolecular Chemistry,  
41 A Grigore Ghica Voda Alley, 700487, Iasi, Roumania

<sup>b</sup> Department of Physical Chemistry of Polymers, Petru Poni Institute of Macromolecular Chemistry,  
41 A Grigore Ghica Voda Alley, 700487, Iasi, Roumania

Received February 26, 2025

Ethylene brassylate (EB) is a renewable macrolactone that can be polymerized via ring-opening polymerization (ROP) to obtain a fully biosourced biodegradable polyester. In this work, a novel synthesis of poly(ethylene brassylate) (PEB) in a homogeneous 1,4-dioxane system at 105 °C is disclosed. The polymerizations were carried out in the presence of two organic catalysts, namely *p*-toluenesulfonic acid (PTSA) and 1,5,7-triazabicyclo[4.4.0]dec-5-ene (TBD), using 1-hexanol as initiator. The obtained PEB aliphatic polyesters were characterized by GPC, FTIR, <sup>1</sup>H NMR, WAXD, TGA, and DLS. Homopolymers showed molecular weights ranging from 1.224 to 2.031 g/mol and polydispersity indices ranging from 1.21 to 1.67. The combination of 1-hexanol/TBD proved to be the fastest system for promoting ROP of EB, leading to polyesters with  $M_w = 1.420$  at EB:TBD molar ratio of 50:1. The DLS investigation revealed that the samples have dimensions in the range of 235–400 nm. The zeta potential values indicated a decrease in colloidal stability with increasing TBD catalyst content. These properties make PEB an interesting aliphatic polyester alternative for the synthesis of polymeric nano- or microparticles, particularly as delivery systems for hydrophobic drugs.



### INTRODUCTION

The increasing global concerns about the environmental consequences of traditional petroleum-based polyolefin materials have accelerated the development of more sustainable

alternatives, including biobased polymers derived from renewable resources. Compared with conventional polymers, the most important advantage of biobased polymers is the renewability of raw materials.<sup>1</sup> Of all biobased polymers, aliphatic polyesters have been extensively studied

\* Corresponding author: lnazare@icmpp.ro

as an important class of biodegradable and biocompatible materials for applications in the fields of healthcare and packaging.<sup>2</sup>

An example of an aliphatic polyester is poly(ethylene brassylate) (PEB), which is a relatively unexplored polymer. Like most aliphatic polyesters, PEB is biodegradable, making it an attractive option for applications where environmental sustainability is a priority or medical applications. Due to its long-chain aliphatic structure, PEB exhibits hydrophobicity with low water reduction and is more resistant to hydrolytic degradation, compared to shorter-chain aliphatic polyesters such as poly(lactic acid) (PLA). Additionally, PEB's biocompatibility makes it a promising material for medical uses, including the development of carriers in tissue engineering. PEB is synthesized via ring-opening polymerization (ROP) of ethylene brassylate (EB), a 17 member ring lactone with two ester groups commercially produced from the condensation reaction of ethylene glycol and 1,13-tridecandioic acid.<sup>3</sup> The latter derives from castor oil, a low-cost renewable source.<sup>4</sup> ROP of EB has been carried out at a lab scale through enzymatic,<sup>5</sup> organometallic,<sup>3</sup> or organic catalysis.<sup>6</sup> Compared to metallic ones, organic catalysts have demonstrated reduced toxicity and environmental impact, relatively lower price than enzymatic alternatives, and they are suitable for the synthesis of polymers for medical applications.<sup>7</sup>

In 2014, Pascual *et al.*<sup>6</sup> were the first to report the use of organic catalysts for the polymerization of EB in bulk and solution conditions (toluene) at 80 °C, with benzyl alcohol serving as the initiator. The polymerizations were carried out in the presence of three acidic catalysts (dodecylbenzenesulfonic acid (DBSA), diphenyl phosphate (DPP), *p*-toluenesulfonic acid (PTSA)) and three basic catalysts (1,5,7-triazabicyclo[4.4.0]dec-5-ene (TBD), 1,2,3-tricyclohexylguanidine (TCHG), and 1,2,3-triisopropylguanidine (TIPG)). The superbase TBD exhibited the highest polymerization efficiency, the fastest reaction rate, the highest molecular weight, and the narrowest polydispersity index value among all compared conditions. The same research group did impressive pioneering works in their study of PEB, including utilizing TBD as both the initiator and the catalyst of the ROP of EB.<sup>8</sup>

From a green chemistry perspective, one of the current challenges in the synthesis of PEB aliphatic polyesters is the use of more environmentally

friendly solvents. To address this, the present work explores an alternative strategy to replace traditional solvents like toluene, chloroform, or diethyl ether. The novelty of this research is the organocatalyzed ROP of EB macro(di)lactone in a homogeneous 1,4-dioxane system. 1,4-dioxane is an organic solvent with a low dielectric constant, preventing appreciable charge removal or significant dissociation of the formed catalytic complex. Likewise, in this kind of synthesis low molecular weight alcohols are commonly used in order to control the molecular weight of the polyesters.<sup>3,9</sup> In our case, 1-hexanol was added to the reaction mixture. Unlike Pascual *et al.*,<sup>6,8</sup> who purified the crude polymer by dissolving it in dichloromethane (10 wt% solution) and precipitating it with cold diethyl ether (1:5), in this work our group proposed purifying the reaction product through repeated wash-sedimentation cycles in cold distilled water. The obtained homopolymers were then characterized by gel permeation chromatography (GPC), Fourier transform infrared spectroscopy (FTIR), proton nuclear magnetic resonance (<sup>1</sup>H NMR), thermogravimetric analysis (TGA), and wide angle X-ray diffraction (WAXD). Literature studies indicate that polyesters can be successfully used to obtain nano- or microparticles for the encapsulation of hydrophobic bioactive compounds.<sup>10-13</sup> Considering these aspects and our goal of developing carriers for hydrophobic drugs, we conducted preliminary experiments to produce microparticles based on PEB due to its combination of flexibility, biodegradability, hydrophobicity, and renewability, making it an excellent choice for sustainable and high-performance material applications. These were analyzed using the dynamic light scattering (DLS) technique. To our knowledge, this is the first report of microparticles based on PEB homopolymer.

## RESULTS AND DISCUSSION

In this work, the ROP of EB in solution was investigated using 1-hexanol as initiator and either PTSA or TBD as organic catalysts, shown in Fig. 1. Briefly, the 1-hexanol is deprotonated by the catalyst, favoring the generation of a carbonate prior to the opening of the macrolactone and the formation of an alkoxide in the brassylate. Subsequent protonation resulted in the production of the terminal alcohol and recovery of the catalyst.

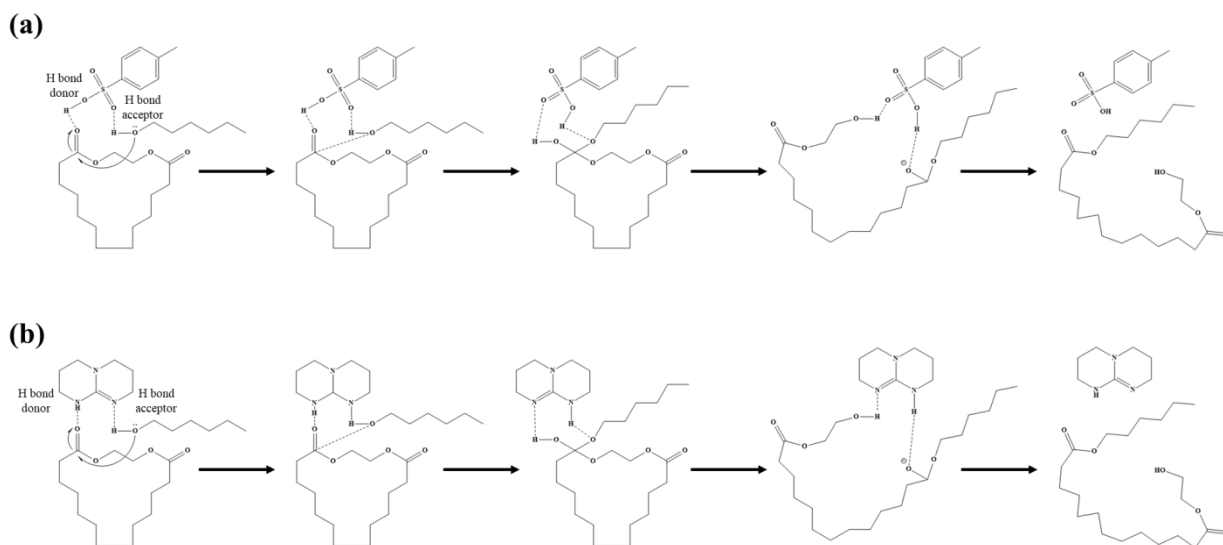


Fig. 1 – Activation mechanism of PTSA (a) and TBD (b) schemes according to Pascual *et al.*<sup>6,8</sup>

Table 1 summarizes the polymerization conditions and the results we obtained. Quantitative conversions determined by the gravimetric method were obtained in all cases.

The obtained PEB had molecular weights between 1.224 and 2.031 g/mol, with relatively low polydispersity indices between 1.21 and 1.67 (Table 2).

Table 1  
Polymerization conditions and results of ethylene brassylate ROP.

Sample	Catalyst	EB:Catalyst (equiv.)	Conversion (%)	Monomer (mol L <sup>-1</sup> )
EB:PTSA=50:1	PTSA	50:1	70.833	0.269
EB:TBD=50:1	TBD	50:1	82.75	0.159
EB:TBD=100:1	TBD	100:1	78.5	0.225
EB:TBD=100:1 without 1-Hexanol	TBD	100:1	77.833	0.209
EB:TBD=150:1	TBD	150:1	76.667	0.228

Table 2  
Molecular weights of the PEB homopolymers.

Sample	M <sub>n</sub> (g/mol)	M <sub>w</sub> (g/mol)	M <sub>z</sub> (g/mol)	M <sub>p</sub> (g/mol)	PDI
EB:TBD=50:1	1.134	1.420	1.725	1.362	1.25
EB:TBD=100:1	1.205	1.463	1.711	1.548	1.21
EB:TBD=100:1 without 1-Hexanol	1.212	2.031	2.954	2.451	1.67
EB:TBD=150:1	970.9	1.224	1.533	1.195	1.26

M<sub>n</sub>: number average molecular weight, M<sub>w</sub>: weight average molecular weight, M<sub>z</sub>: higher average molecular weights, M<sub>p</sub>: molecular weight of the highest peak, PDI: polydispersity index.

The effects of the type of organic catalyst used, the monomer to initiator and catalyst ratios, and 1-hexanol as initiator were investigated and discussed in the following sections.

### Effects of the presence of the organic catalyst

Conversion kinetic results are plotted in Fig. 2. Experimentally, it is found that the polymerization rate of EB is accelerated in the presence of TBD,

while in the presence of PTSA, the process becomes much more complex. The differences in polymerization rates are linked to the ability of the catalyst to activate the species, which primarily depends on their electrophilic or nucleophilic character (for acids and bases, respectively).<sup>6</sup> Although PTSA is a strong sulfonic acid (pK<sub>a</sub> = -2.8), it initially acts as an inhibitor but transitions into behaving as a retarder after the induction period ends. In principle, the difference

between inhibition and retardation is fundamentally kinetic and does not concern the mechanism, which in both cases involves a chain transfer. On the other hand, TBD is well-known as a strong superbase with  $pK_a \sim 21$ , making it the fastest catalyst for ROP. Finally, both reactions achieved over 70% conversion within 24 h.

### Effect of monomer concentration

To evaluate the influence of monomer concentration on the polymerization rate, three monomer:TBD molar ratios (50:1, 100:1, and 150:1) were investigated. In all cases, the polymerization can be roughly divided into two stages. A first stage in which the polymerization follows a first-order kinetic and a second stage (conversion above 50%) in which the monomer

diffusion limitation slows down the reaction. Increasing the monomer-to-catalyst molar ratio to 150:1 (EB:TBD=150:1) resulted in lower molecular weights than expected. This can be attributed to the slow diffusion of the monomer and the reduced amount of catalyst. As the polymerization process progresses, the system's viscosity increases, leading to a reduced diffusion rate of macroradicals and, consequently, a lower probability of their collision, which is necessary for stabilization. Surprisingly, a conversion of 77% was achieved even without 1-hexanol, along with higher molecular weights. Molecular weights of 2.031 g/mol were obtained without any catalyst, in comparison to 1.463 g/mol with catalyst. Looking at these results, it is confirmed that TBD participates in the polymerization process as a catalyst and also as an initiator.<sup>8</sup>

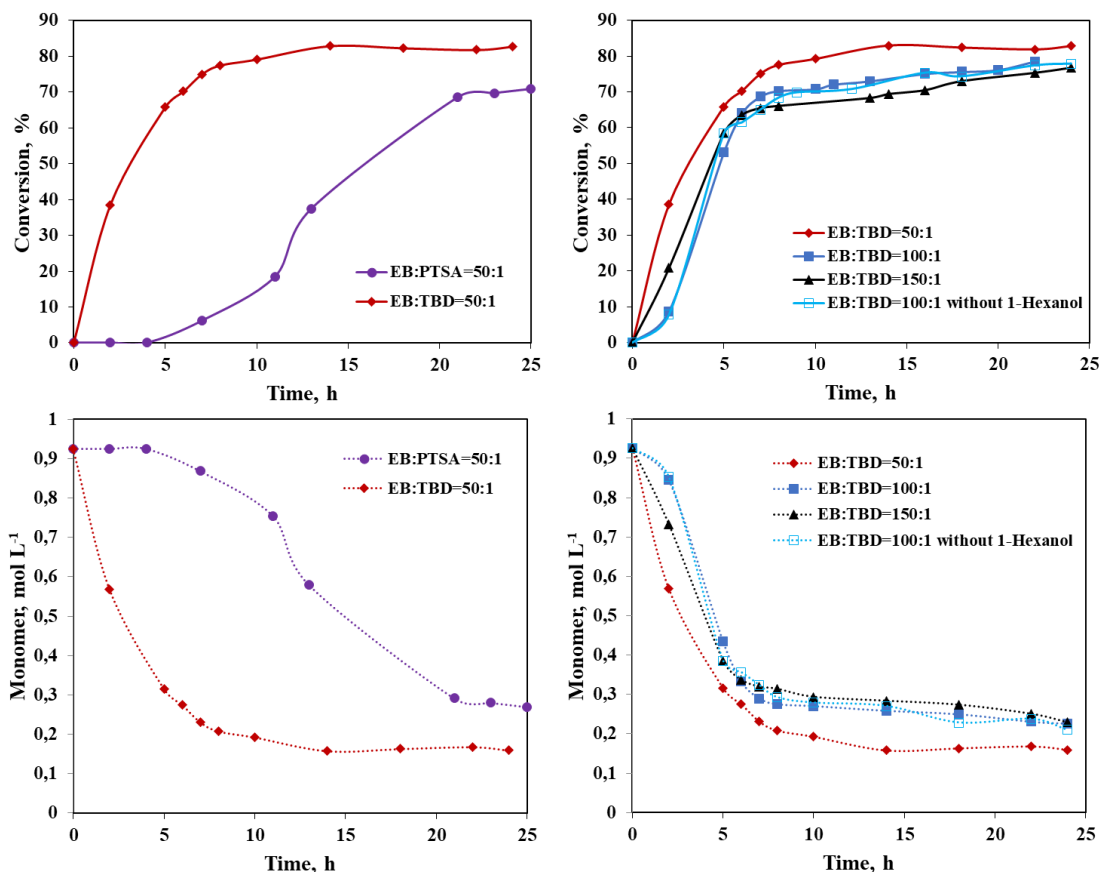


Fig. 2 – Monomer conversion as a function of reaction time.

### Structural characterization

FTIR characterization was employed to confirm the structure of the obtained homopolymer. The spectrum of EB:TBD=50:1 (Fig. 3a) shows peaks corresponding to the EB monomer as well as the

changes resulting from the opening of the macrolactone cycle, which are also registered in the spectrum. The signals at 2925, 2856, and 1459  $\text{cm}^{-1}$  are attributed to the asymmetric, symmetric stretching, and bending vibrations of C–H bonds. The presence of C=O bonds in the homopolymer

structure is confirmed by the strong peak observed at  $1737\text{ cm}^{-1}$ . Additional distinctive bands are found in the range of  $1100\text{--}1300\text{ cm}^{-1}$ , corresponding to the stretching vibrations of C–O bonds. Furthermore, the appearance of the signal at  $3455\text{ cm}^{-1}$ , corresponding to the –OH group at the end of the polymer chain, confirms the success of the PEB synthesis.

The  $^1\text{H NMR}$  spectra of the synthesized homopolymer illustrated in Fig. 3b support the FTIR data, confirming the chemical structure. The spectra present characteristic signals assigned to PEB at: 4.26 ppm (s,  $\text{CH}_2\text{O}$ –a), 2.31 ppm (t,  $\text{CH}_2\text{C}=\text{O}$ –b), 1.61 ppm (m,  $\text{CH}_2$ –c), 1.28 ppm (m,  $\text{CH}_2$ –d), 3.82 ppm (t,  $\text{CH}_2$ –OH–e), and 0.88 ppm (t,  $\text{CH}_3$ –f), these corresponding to the notation of the protons identified in the structure. The synthesis is confirmed by the presence of signals e and f, assignable to  $\alpha$ -methylene protons of the – $\text{CH}_2\text{OH}$  end group at 3.82 ppm and the methylene protons of 1-hexanol initiator residue at 0.88 ppm. The repeating units of EB are confirmed by the presence of chemical shifts at 2.31 ppm (b), 1.61 ppm (c), 1.28 ppm (d), and 4.26 ppm (a).

The experimental numerical molecular weight  $M_n = 6.15\text{ kgmol}^{-1}$ , was determined using  $^1\text{H NMR}$  spectroscopy.<sup>6</sup> This was achieved by analyzing the ratio between the integrals of the proton signals of the repeating units – $\text{C}(=\text{O})\text{OCH}_2$  in the polymer chains (at 4.30 ppm) and the  $\alpha$ -methylene protons of the terminal group – $\text{CH}_2\text{OH}$  at 3.68 ppm. The conversion rate was calculated by determining the ratio between the integrals of the proton signals of the repeating units – $\text{C}(=\text{O})\text{OCH}_2$  in the polymer chains and the corresponding EB monomer (a (4.30 ppm) and a' (4.34 ppm)). Thus, the peak at 4.34 ppm, which corresponds to the EB monomer) (Fig. 3) is no longer visible on the  $^1\text{H NMR}$  spectrum. This observation supports the conclusion, as confirmed by Pascual and collaborators,<sup>6,8</sup> that the conversion exceeds 90%. This finding is also in agreement with the polymerization kinetics data presented previously.

All these data are in good agreement with the literature data on previously reported PEB homopolymers, supporting the similar chemical structure of the homopolymer synthesized through different methods.<sup>6–8,14</sup>

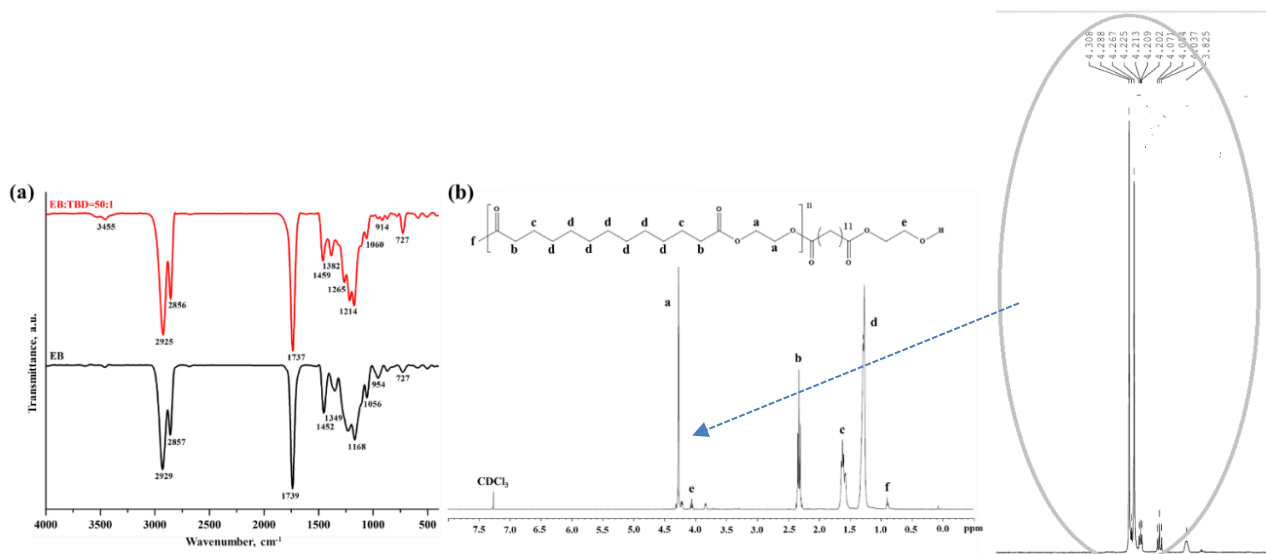


Fig. 3 – FTIR (a) and  $^1\text{H NMR}$  (b) spectra of PEB.

Further information on the crystal structure and degree of crystallinity of PEB was obtained from WAXD measurements. Figure 4 shows the diffraction profile of the homopolymer obtained compared with the diffractogram of the reference monomer (EB). As can be seen, EB did not present an obvious diffraction peak, indicating its amorphous state due to its low crystallization ability. The PEB diffractogram showed two sharp characteristic diffraction

peaks at  $2\theta = 21.43^\circ$  ( $d = 4.14\text{ \AA}$ ) and  $23.95^\circ$  ( $d = 3.71\text{ \AA}$ ), and two small peaks at  $2\theta = 30.02^\circ$  ( $d = 2.97\text{ \AA}$ ) and  $35.94^\circ$  ( $d = 2.50\text{ \AA}$ ), data mentioned also by other authors.<sup>3,15–17</sup> WAXD analysis again confirms the chemical structure of the synthesized homopolymer. The degree of crystallinity is approximately 57.2%. The average crystallite size calculated with the Scherrer equation was estimated to be 25.3 nm (FWHM=0.3%).

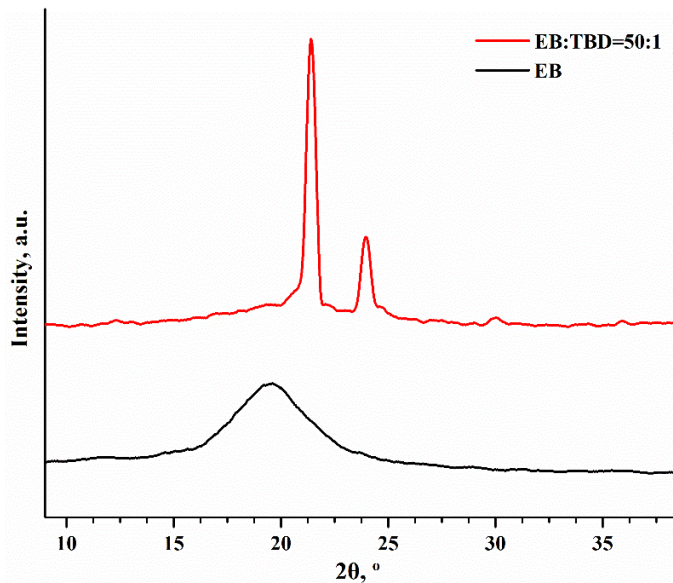


Fig. 4 – WAXD patterns of PEB and EB monomer.

### Thermal characterization

Table 3 presents the main parameters characterizing the thermal behavior of PEB. The recorded TG and DTG curves are shown in Fig. 5. The thermogravimetric analysis reveals a single-step decomposition process, with the maximum degradation temperature ( $T_{\text{peak}}$ ) at approximately 454 °C and a residual mass of 1.16%. This result is consistent with

data reported in the literature.<sup>3,6</sup> As reported in a previous study,<sup>3</sup> the PEB homopolymer synthesized using the TBD catalyst also underwent single-step thermal degradation, with a final degradation temperature of 460 °C. The polymerization mechanism associated with TBD catalysis is believed to promote the formation of more ordered structures that are free of metallic residues, in contrast to polymers obtained using triphenyl bismuth as a catalyst.

Table 3

Main degradation parameters depicted for PEB

Degradation stage	$T_{\text{onset}}$ (°C)	$T_{\text{peak}}$ (°C)	$T_{10}$ (°C)	$T_{20}$ (°C)	W (%)	Residual mass (%)
I	393.6	454.1	398	420	98.84	1.16

$T_{\text{onset}}$ : the temperature at which the thermal degradation begins,  $T_{\text{peak}}$ : the temperature at which the degradation rate is maximum,  $T_{10}$ ,  $T_{20}$ : temperatures corresponding to 10% and 20% mass losses, W: mass losses.

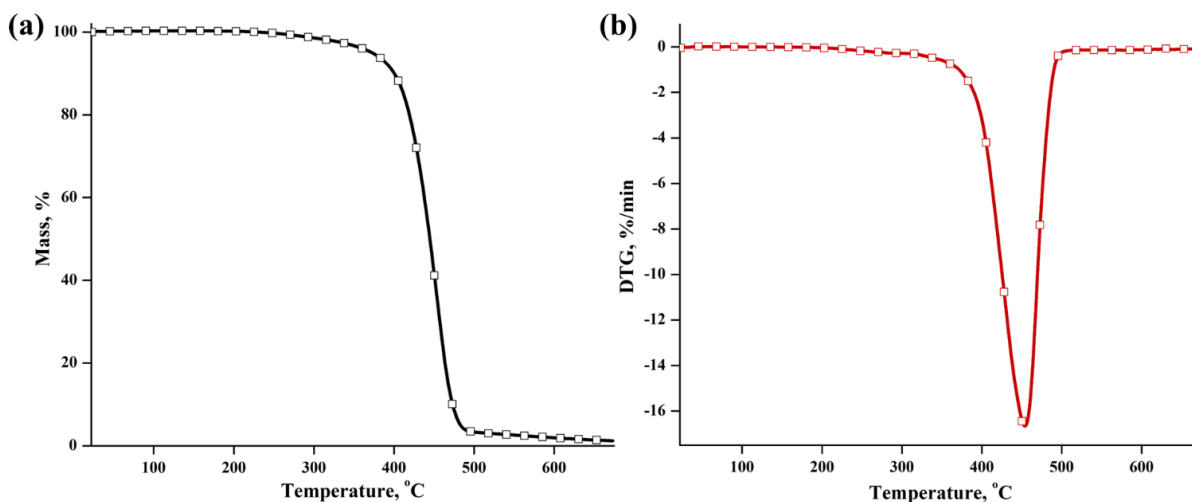


Fig. 5 – TG (a) and DTG (b) curves of PEB.

## DLS investigations

The interest in the dimensional evaluation of the synthesized homopolymer arises mainly from its intended use as a polymeric network for the incorporation of a hydrophobic bioactive compound, a process that preferably occurs in solution. To gain a deeper understanding of its behavior in an aqueous state, DLS investigations were employed. Figure 6 illustrates the size distribution of the PEB variants. Table 4 presents the main DLS parameters, namely the hydrodynamic diameter ( $D_H$ ) and zeta potential (ZP) of the samples. EB:TBD=50:1 presented a monomodal size distribution, with the smallest hydrodynamic diameter of the main peak at

234.2 nm, a value close to the nanometric range of approximately 200 nm. The other two variants showed a bimodal distribution, with hydrodynamic diameters up to 400 nm: 399.6 nm for EB:TBD=100:1 and 327.6 nm in the case of the EB:TBD=150:1 sample. The ZP values indicate a decrease in colloidal stability with increasing TBD catalyst content (Table 4).

The DLS data suggest that the EB:TBD=50:1 variant is the most suitable for future medical applications, aiming to obtain nano- or microparticles capable of incorporating hydrophobic compounds. These results are also supported by conversion studies, which showed a monomer-to-polymer transformation of approximately 83% for the same sample.

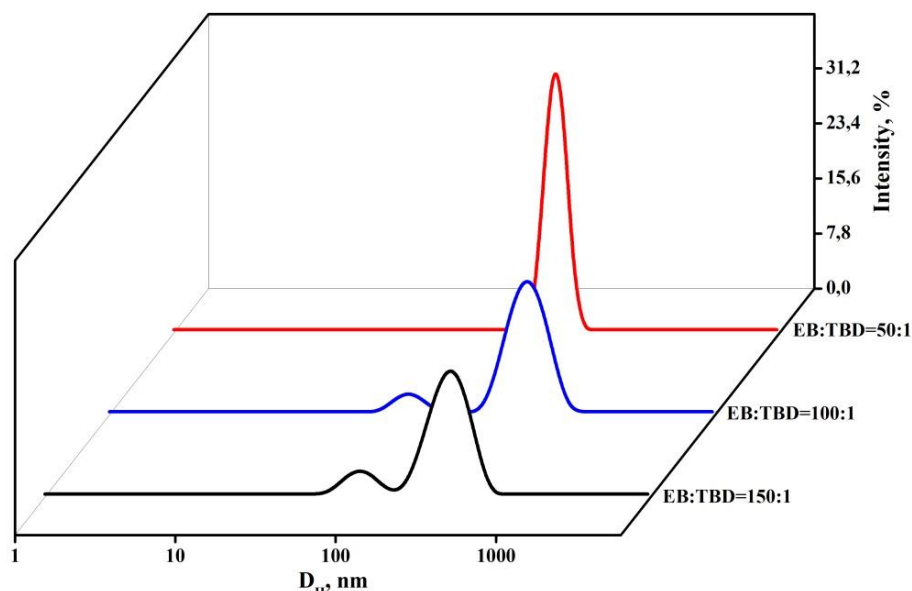


Fig. 6 – Size distribution of the samples.

Table 4

DLS parameter values determined for samples.

Sample	$D_H^*$ (nm)	ZP (mV)
EB:TBD=50:1	234.2	-21.6
EB:TBD=100:1	399,6	-10
EB:TBD=150:1	327.6	-0.206

\* measured according to the main peak

## EXPERIMENTAL

### Materials

Ethylene brassylate (EB, 1,4-dioxacycloheptadecane-5,17-dione,  $C_{15}H_{26}O_4$ ,  $M_w = 270.36$  g/mol,  $\geq 95\%$ ), *p*-toluenesulfonic acid (PTSA,  $CH_3C_6H_4SO_3H \cdot H_2O$ ,  $M_w = 190.22$  g/mol,  $\geq 98.5\%$ ),

1,5,7-triazabicyclo[4.4.0]dec-5-ene (TBD,  $C_7H_{13}N_3$ ,  $M_w = 139.20$  g/mol, 98%), and 1,4-dioxane ( $\geq 99.0\%$ ) were purchased from Sigma-Aldrich (Steinheim, Germany); anhydrous 1-hexanol ( $H_3C(CH_2)_4CH_2OH$ , 99%) was acquired from Acros Organics (Geel, Belgium), and acetone ( $CH_3COCH_3$ , 99.9%) from Chimreactiv (Bucuresti, Roumania). All chemicals were used as received without further purification.

## Homopolymerization of EB

New variants of PEB homopolymer were synthesized by one-pot one-step ROP in a homogeneous 1,4-dioxane system, using 1-hexanol as the initiator and either PTSA or TBD as the catalyst. The reactions were conducted over 24 h in a flask immersed in a temperature-controlled oil bath at 105 °C, under a nitrogen atmosphere, with a stirring rate of 250 rpm. A typical experiment for the EB:TBD=100:1 variant (Table 1) involves 11.52 mL EB (44.38 mmol, 100 equiv.), 0.0617 g TBD (0.4438 mmol, 1 equiv.), 0.6 mL 1-Hexanol, and 48 mL 1,4-dioxane. To evaluate monomer conversion, aliquots were collected at different time intervals and precipitated in cold distilled water and acetone solution (2:1). The precipitate was filtered and dried at room temperature, and the conversion was determined using the gravimetric method. After the corresponding reaction time, the product was purified through repeated wash-sedimentation cycles in cold distilled water. The resulting product was then freeze-dried for further characterization (Martin Christ Apha 2-4 LSCplus, Osterode am Harz, Germany).

## Characterization methods

### GPC analysis

The molecular weights of the samples were determined by GPC instrument WGE SEC-3010 multi-detection system (Brookhaven, GA, USA), with two PLgel columns (PLgel 5micro Mixed C and PLgel 5micro Mixed D), and a dual refractometer/viscometer (RI/VI) detector. The working solutions were prepared in chloroform (4 mg/mL CHCl<sub>3</sub>) and the measurements were conducted at a flow rate of 1.0 mL/min at 30 °C. The RI/VI detector was calibrated with polystyrene standards (580-1.350.000 Da) with a narrow molecular weight distribution. Data acquisition and analysis were achieved using ParSEC Chromatography v 5.67 software.

### Structural analysis

**FTIR** spectra of the samples were obtained using a Bruker Vertex 70 Spectrometer (Ettlingen, Germany). The potassium bromide disk method was used for sample preparation: 1 mg of dried sample was mixed with potassium bromide powder and compressed into a disk shape. The spectra were recorded in transmittance mode over the range of

4000 to 400 cm<sup>-1</sup>, with a resolution of 4 cm<sup>-1</sup> and an average of 64 scans.

**<sup>1</sup>H NMR** experiment was accomplished in solution-state at 400.1 MHz on a Bruker Neo Instrument spectrometer from Bruker BioSpin (Rheinstetten, Germany). The sample was solubilized in deuterated chloroform (CDCl<sub>3</sub>) and transferred in a 5 mm multinuclear inverse detection z-gradient probe. Spectra were recorded at room temperature, with chemical shifts reported in  $\delta$  units (ppm) and referenced to the solvent peak at 7.26 ppm. <sup>1</sup>H NMR (400.1 MHz, CDCl<sub>3</sub>,  $\delta$ , ppm): 4.26 (s, CH<sub>2</sub>O-a), 2.31 (t, CH<sub>2</sub>C=O-b), 1.61 (m, CH<sub>2</sub>-c), 1.28 (m, CH<sub>2</sub>-d), 3.82 (t, CH<sub>2</sub>-OH-e), and 0.88 (t, CH<sub>3</sub>-f).

**WAXD** was recorded on a Diffractometer D8 ADVANCE (Bruker AXS, Germany), using a SIEMENS KFL Cu 2K tube, with the Cu-K $\alpha$  radiation ( $\lambda = 0.1506$  nm), a parallel beam with Gobel mirror and a Dynamic Scintillation detector. The working conditions were: Locked Coupled Scan type / step scan; 36 kV and 35 mA emission current; scan speed: time/step 2s/step, 0.02 degree/step increment. All the diffractograms were investigated in the range 5-80° (2 theta degrees), at 24 °C working temperature. Bruker Soft: DIFFRAC Plus Commander for data acquisition; DIFFRAC-Evaluation: Eva and File Exchange for data processing: numerical values for 2 theta angle (°),  $d$  interplanar distance (Angstrom), Intensity (cps), Relative Intensity (%), Crystallite size (nm), Degree of crystallinity (%). The degree of crystallinity (%) was determined using the ratio of the crystalline peak areas to the total area under the diffraction curve, while the average crystallite size (nm) was obtained employing the Scherrer Equation (1).<sup>18</sup> The latter data were calculated from the most intense peaks in the diffraction pattern: at  $2\theta = 21.4^\circ$ :

$$D = \frac{K\lambda}{\beta \cos\theta} \quad (1)$$

where  $K$  is the Scherrer constant (0.9),  $\lambda$  is the X-ray wavelength,  $\beta$  is the full width at half maximum (FWHM) of the peak at  $2\theta$  in radians, and  $\theta$  is the Bragg angle.

### Thermogravimetric analysis (TGA and DTG)

The thermal properties of the synthesized homopolymer were investigated on a Jupiter STA 449 F1 thermobalance from Netzsch (Selb, Germany). 15 mg of freeze-dried sample was placed in an open Al<sub>2</sub>O<sub>3</sub> crucible and heated in a nitrogen atmosphere (40 mL/min gas flow) up to 675 °C. The measurements were performed in dynamic mode with a heating rate of 10 °C/min, and data

acquisition was processed using Proteus v 5.0.1 software.

### DLS measurements

Size determinations of the samples were made with the DLS technique using a Zetasizer Nano ZS device from Malvern Panalytical (Worcestershire, UK), equipped with a 633 nm wavelength red laser (He/Ne). The system uses a non-invasive back scatter (NIBS) technology (which reduces the multiple scattering effects), wherein the optics are not in contact with the sample, back scattered light being detected. The hydrodynamic diameter was calculated using the Stokes-Einstein Equation (2):

$$D_H = \frac{kT}{3\pi\eta D} \quad (2)$$

where  $D_H$  is the hydrodynamic diameter,  $k$  is the Boltzmann constant,  $T$  is the temperature,  $\eta$  is the viscosity, and  $D$  is the diffusion coefficient.

ZP was determined on the same apparatus using the Smoluchowski Equation (3):

$$\zeta = \frac{\eta\mu}{\varepsilon} \quad (3)$$

where  $\eta$  is the viscosity,  $\mu$  is the electrophoretic mobility, and  $\varepsilon$  represents the dielectric constant of the medium.

## CONCLUSIONS

PEB is a little-known polyester that holds a significant interest in the medical field and for eco-friendly applications due to the low cost of its monomer compared to other lactones and macrolactones. The synthesis of PEB presented in this study aims to move toward more sustainable practices, focusing on improving reaction efficiency, minimizing resource use, and targeting biomedical applications that justify the selection of current reagents. PEBs were synthesized in solution using 1-hexanol as an initiator and either PTSA or TBD as catalysts, in 1,4-dioxane as solvent. Although these reagents are not inherently green, their use in small amounts, under mild conditions, and in high-yielding reactions helps reduce waste and energy consumption. Homopolymers with molecular weights ranging from 1.224 to 2.031 g/mol and polydispersity indices between 1.21 and 1.67 were obtained. The combination of

1-hexanol/TBD proved to be the fastest system to promote the ROP of EB, leading to polyesters with  $M_w = 1.420$  g/mol at EB:TBD molar ratio of 50:1. The performed spectroscopic analyses, FTIR and  $^1\text{H}$  NMR, confirmed the chemical structure of the homopolymer. The degree of crystallinity from the WAXD investigation was approximately 57.2%, and the average crystallite size was estimated at 25.3 nm. Thermogravimetric analysis revealed that the thermal decomposition proceeded through a single-step mechanism, with a maximum degradation temperature of approximately 454 °C and a residual mass of 1.16%, indicating good thermal stability of the polymeric material. The DLS data indicate that the EB:TBD=50:1 variant is the most appropriate for future medical applications focused on obtaining nano- or microparticles capable of incorporating hydrophobic bioactive compounds. These findings are also validated by conversion studies, which revealed a monomer-to-polymer transformation of about 83% for the same sample. Studies are ongoing for the incorporation of norfloxacin, a broad-spectrum antibiotic, in order to demonstrate the applicability of the polymeric system.

## REFERENCES

1. C. Jin, Z. Wei, Y. Yu, M. Sui, X. Leng and Y. Li, *Eur. Polym. J.*, **2018**, *102*, 90–100.
2. Z. Wei, C. Jin, Q. Xu, X. Leng, Y. Wang and Y. Li, *J. Mech. Behav. Biomed. Mater.*, **2019**, *91*, 255–265.
3. J. Fernández, H. Amestoy, H. Sardon, M. Aguirre, A. L. Varga and J. R. Sarasua, *J. Mech. Behav. Biomed. Mater.*, **2016**, *64*, 209–219.
4. S. F. Marxsen, D. Song, X. Zhang, I. Flores, J. Fernández, J. R. Sarasua, A. J. Müller and R. G. Alamo, *Macromolecules*, **2022**, *55*, 3958–3973.
5. S. Namekawa, S. Suda, H. Uyama and S. Kobayashi, *Int. J. Biol. Macromol.*, **1999**, *25*, 145–151.
6. A. Pascual, H. Sardon, A. Veloso, F. Ruipérez and D. Mecerreyes, *ACS Macro Lett.*, **2014**, *3*, 849–853.
7. A. Avella, A. Rafi, L. Deiana, R. Mincheva, A. Córdova and G. Lo Re, *ACS Sustainable Chem. Eng.* **2024**, *12*, 10727–10738.
8. A. Pascual, H. Sardon, F. Ruipérez, R. Gracia, P. Sudam, A. Veloso and D. Mecerreyes, *J. Polym. Sci. Part A: Polym. Chem.*, **2015**, *53*, 552–561.
9. J. Fernández, E. Meaurio, A. Chaos, A. Etxeberria, A. Alonso-Varona and J. R. Sarasua, *Polymer*, **2013**, *54*, 2621–2631.
10. J. C. Chen, J. Z. Li, J. H. Liu and L. Q. Xu, *Chin. Chem. Lett.* **2015**, *26*, 1319–1321.
11. V. Korzhikov, I. Averianov, E. Litvinchuk and T. B. Tennikova, *J. Microencapsul.*, **2016**, *33*, 199–208.

12. K. Walker, J. F. Stumbé and R. Haag, *Polymers*, **2016**, *8*, 192.
13. T. Slomkowski, M. Basinska, M. Gadzinowski and D. Mickiewicz, *Polymers*, **2024**, *16*, 2503.
14. S. Kim and H. Chung, *ACS Sustainable Chem. Eng.*, **2021**, *9*, 14766–14776.
15. J. Fernández, A. Larrañaga, A. Etxeberria and J. R. Sarasua, *RSC Adv.*, **2016**, *6*, 22121–22136.
16. C. Jin, X. Leng, M. Zhang, Y. Wang, Z. Wei and Y. Li, *Polym. Int.*, **2020**, *69*, 363–372.
17. W. Sartillo-Bernal, R. Yáñez-Macías, R. López-González, J. F. Lara-Sánchez, J. Gudiño-Rivera and H. A. Fonseca-Florido, *J. Polym. Environ.*, **2024**, *32*, 6603–6617.
18. P. Scherrer, “Bestimmung der Größe und der inneren Struktur von Kolloidteilchen mittels Röntgenstrahlen”, 1918, pp. 98–100.